World Journal of Clinical Cases

Submit a Manuscript: https://www.f6publishing.com

World J Clin Cases 2023 July 16; 11(20): 4852-4864

DOI: 10.12998/wjcc.v11.i20.4852

ISSN 2307-8960 (online)

ORIGINAL ARTICLE

Retrospective Study

Diagnostic value of preoperative examination for evaluating margin status in breast cancer

Peng Liu, Ye Zhao, Dong-Dong Rong, Kai-Fu Li, Ya-Jun Wang, Jing Zhao, Hua Kang

Specialty type: Surgery

Provenance and peer review: Unsolicited article; Externally peer-reviewed.

Peer-review model: Single-blind

Peer-review report's scientific quality classification

Grade A (Excellent): 0
Grade B (Very good): 0
Grade C (Good): C, C
Grade D (Fair): 0
Grade E (Poor): 0

P-Reviewer: Gounden SM, South Africa; Janelsins M, United States

Received: May 11, 2023
Peer-review started: May 11, 2023
First decision: May 31, 2023
Revised: June 8, 2023
Accepted: June 21, 2023
Article in press: June 21, 2023
Published online: July 16, 2023

Peng Liu, Ye Zhao, Kai-Fu Li, Ya-Jun Wang, Jing Zhao, Hua Kang, Department of General Surgery, Center for Thyroid and Breast Surgery, Xuanwu Hospital, Capital Medical University, Beijing 100053, China

Peng Liu, Department of General Surgery, Beijing Fengtai Hospital, Beijing 100071, China

Dong-Dong Rong, Department of Radiology, Xuanwu Hospital, Capital Medical University, Beijing 100053, China

Corresponding author: Hua Kang, MD, Chief Doctor, Department of General Surgery, Center for Thyroid and Breast Surgery, Xuanwu Hospital, Capital Medical University, No. 45 Changchun Street, Xicheng District, Beijing 100053, China. kanghua@xwh.ccmu.edu.cn

Abstract

BACKGROUND

A positive resection margin is a major risk factor for local breast cancer recurrence after breast-conserving surgery (BCS). Preoperative imaging examinations are frequently employed to assess the surgical margin.

AIM

To investigate the role and value of preoperative imaging examinations [magnetic resonance imaging (MRI), molybdenum target, and ultrasound] in evaluating margins for BCS.

METHODS

A retrospective study was conducted on 323 breast cancer patients who met the criteria for BCS and consented to the procedure from January 2014 to July 2021. The study gathered preoperative imaging data (MRI, ultrasound, and molybdenum target examination) and intraoperative and postoperative pathological information. Based on their BCS outcomes, patients were categorized into positive and negative margin groups. Subsequently, the patients were randomly split into a training set (226 patients, approximately 70%) and a validation set (97 patients, approximately 30%). The imaging and pathological information was analyzed and summarized using R software. Non-conditional logistic regression and LASSO regression were conducted in the validation set to identify factors that might influence the failure of BCS. A column chart was generated and applied to the validation set to examine the relationship between pathological margin range and prognosis. This study aims to identify the risk

factors associated with failure in BCS.

RESULTS

The multivariate non-conditional logistic regression analysis demonstrated that various factors raise the risk of positive margins following BCS. These factors comprise non-mass enhancement (NME) on dynamic contrast-enhanced MRI, multiple focal vascular signs around the lesion on MRI, tumor size exceeding 2 cm, type III time-signal intensity curve, indistinct margins on molybdenum target examination, unclear margins on ultrasound examination, and estrogen receptor (ER) positivity in immunohistochemistry. LASSO regression was additionally employed in this study to identify four predictive factors for the model: ER, molybdenum target tumor type (MT Xmd Shape), maximum intensity projection imaging feature, and lesion type on MRI. The model constructed with these predictive factors exhibited strong consistency with the real-world scenario in both the training set and validation set. Particularly, the outcomes of the column chart model accurately predicted the likelihood of positive margins in BCS.

CONCLUSION

The proposed column chart model effectively predicts the success of BCS for breast cancer. The model utilizes preoperative ultrasound, molybdenum target, MRI, and core needle biopsy pathology evaluation results, all of which align with the real-world scenario. Hence, our model can offer dependable guidance for clinical decision-making concerning BCS.

Key Words: Breast cancer; Breast-conserving surgery; Imaging features; Positive surgical margin; Regression analysis model

Core Tip: This retrospective study analyzed ultrasound, mammography, magnetic resonance imaging (MRI), and biopsy data from enrolled patients and developed a nomogram model to forecast the success of breast-conserving surgery (BCS). This study revealed that estrogen receptor-positive status, mammography tumor type, maximum intensity projection imaging feature, and MRI tumor type were four variables capable of predicting negative margins and influencing the outcome of BCS. The results underwent internal validation and were additionally corroborated *via* calibration curves, indicating a robust correlation between predicted and actual surgical success rates. Overall, this study offers valuable data for assessing the success of BCS in the preoperative phase.

Citation: Liu P, Zhao Y, Rong DD, Li KF, Wang YJ, Zhao J, Kang H. Diagnostic value of preoperative examination for evaluating margin status in breast cancer. *World J Clin Cases* 2023; 11(20): 4852-4864
URL: https://www.wjgnet.com/2307-8960/full/v11/i20/4852.htm
DOI: https://dx.doi.org/10.12998/wjcc.v11.i20.4852

INTRODUCTION

Breast cancer is the most common malignancy and the leading cause of mortality among women[1]. Although numerous prospective clinical studies have shown no statistically significant disparities in overall survival and disease-free survival between breast-conserving surgery (BCS) plus whole-breast radiation therapy and mastectomy for early breast cancer patients, BCS has emerged as the favored surgical approach for early-stage breast cancer[2-4]. Nonetheless, the influence of margin status on postoperative recurrence following BCS remains contentious, as the majority of studies indicate a heightened local recurrence rate in instances with positive margins[5]. Re-excision rates attributable to positive margins following BCS for early breast cancer are considerable, ranging from 10% to 50%, with an average of approximately 20% [6,7]. Consequently, preoperative patient assessment to identify risk factors for postoperative positive margins proves advantageous in circumventing subsequent surgeries.

Currently, a standardized approach to assessing positive margins is lacking. Notably, even when deemed negative by experienced physicians, there exists a minimum local recurrence rate of 10%, primarily in proximity to the surgical site[8, 9]. Therefore, it is imperative to investigate methods of achieving a negative margin and mitigating the risk of recurrence through preoperative evaluation.

This study aims to analyze the clinical and pathological data and follow-up information of breast cancer patients who received BCS treatment at the Thyroid and Breast Disease Diagnosis and Treatment Center of Xuanwu Hospital, Capital Medical University. The study seeks to investigate the association between preoperative breast magnetic resonance imaging, ultrasound, mammography examinations, and imaging information, along with intraoperative and postoperative pathological data. The objective is to enhance the accuracy of preoperative assessment for BCS margins, augment the success rate of the procedure, and uphold a desirable cosmetic outcome.

MATERIALS AND METHODS

Inclusion and grouping of study subjects

This retrospective analysis aimed to assess the correlation between preoperative breast imaging modalities [magnetic resonance imaging (MRI), ultrasound, and mammography] and intraoperative and postoperative pathological data to enhance the precision of preoperative assessment for BCS margins and increase the success rate of the procedure. The study included patients diagnosed with breast cancer through core needle biopsy, who were admitted to the Thyroid and Breast Disease Diagnosis and Treatment Center of Xuanwu Hospital, Capital Medical University, between January 2014 and July 2021. These patients fulfilled the criteria for BCS outlined in the "Clinical Practice Guidelines for High-Resolution Breast PET, 2019 edition" in China and opted for BCS[10]. All patients signed the informed consent for surgery, and with the approval of the Medical Ethics Committee of Xuanwu Hospital, Capital Medical University, we collected the general information of patients, including breast MRI, breast ultrasound, breast mammography, the status of frozen pathology margins during BCS, intraoperative frozen pathology, postoperative paraffin pathology, clinical staging, and other information.

The inclusion criteria encompassed patients who received a breast cancer diagnosis through core needle biopsy, underwent high-resolution breast ultrasound evaluation for suspicious breast nodules and axillary lymph node status assessment prior to surgery, fulfilled the BCS criteria outlined in the "Breast Cancer Diagnosis and Treatment Guidelines (2013 edition)" in China, opted for BCS, and possessed comprehensive preoperative breast MRI, mammography, and ultrasound examination data, alongside complete postoperative pathological records. Please refer to Table 1 for detailed patient information. We excluded patients with collagen vascular diseases, systemic lupus erythematosus, and other relevant medical conditions, individuals with small affected breasts (volume < 200 mL) that may compromise favorable cosmetic outcomes following BCS, those with multiple axillary lymph node metastases, individuals with history of breast or chest wall radiation therapy on the affected side, patients with incomplete postoperative pathological records, and individuals who received preoperative evaluations in other hospitals and lacked the preoperative MRI, ultrasound, and mammography results from our institution.

MRI examination methods and image analysis

A dedicated 4-channel breast coil was used with the Vefa 3.0T MRI scanner (Siemens, Germany). The patient was positioned prone with the head first, allowing both breasts to be naturally suspended within the coil aperture for scanning. All sequences were axial with a 4mm slice thickness. The remaining parameters are as follows: T2-weighted imaging utilized a fast spin echo sequence with frequency selective fat suppression (FOV = 340 mm, TR = 3650 ms, TE = 61 ms, matrix = 314 × 320, bandwidth = 319 Hz). T1-weighted imaging employed a gradient echo sequence utilized a fast spin echo sequence with frequency selective fat suppression (FOV = 340 mm, TR = 3650 ms, TE = 61 ms, matrix = 314 × 320, bandwidth = 319 Hz). Diffusion-weighted imaging employed a spin echo-echo planar imaging sequence (FOV = 340 mm, TR = 9700 ms, TE = 68 ms, matrix = 64 × 132, bandwidth = 2104 Hz) with diffusion coefficients of b-values 400s/mm^2 and 800s/mm^2. Dynamic contrast-enhanced imaging harnessed a three-dimensional volume interpolation method (FOV = 360 mm, TR = 4.67 ms, TE = 1.66 ms, matrix = 296 × 384, slice thickness = 1.2 mm, bandwidth = 320 Hz, scan time = 59 s) with a total of 6 phases and a cumulative time of 5 min 54 s. Mean-Curve software was applied for image processing after the scan. Two radiologists collaboratively reviewed and analyzed the number, morphology, size, edge characteristics, and location of the lesions on plain and enhanced images. They also assessed the enhancement characteristics, surrounding tissue enhancement, and vascular features surrounding the lesions.

The MRI examination was based on the Breast Imaging Reporting and Data System-MRI (BI-RADS MRI) in accordance with the fifth edition of the Magnetic Resonance Imaging Breast Imaging Reporting and Data System (2013)[11]. The main lesion morphology was classified as mass or non-mass enhancement (NME), with attention given to the presence or absence of other lesions in the vicinity of the mass. Additionally, the mass lesion was characterized by its shape (irregular or oval), margin (well-circumscribed, spiculated, indistinct, or lobulated), enhancement pattern (rim enhancement, homogeneous enhancement, or heterogeneous enhancement), and time-intensity curve (type I, type II, or type III). The maximum diameter of the main lesion (MRImd) was recorded as well. In the maximal intensity projection (MIP) image, the vascular features around the lesion were classified as bilateral no enhancement, bilateral symmetric enhancement, unilateral linear enhancement, or unilateral multifocal enhancement, as shown in Figure 1.

Ultrasound examination method and image analysis

The ultrasound examination was performed using the Philip IU 22 diagnostic instrument with a probe frequency of 7-10 MHz, set to breast conditions, and a depth of 3.5-5.0 cm. The patient was placed in a supine position with the arms raised to fully expose the breast and axilla. Two scanning methods were employed: (1) Radially scanning outward from the nipple in clockwise or counterclockwise order; and (2) scanning each section in a cross-sectional and longitudinal manner, moving from top to bottom and left to right. The scanning areas overlapped and encompassed the nipple and the tail of the axillary gland. The examination of axillary lymph nodes involved orderly multi-sectional examinations conducted along the long and short axes of the axilla. The diagnostic information acquired from the examination encompassed the location, shape, boundary, edge, internal and posterior echoes, presence of calcification, and changes in surrounding tissues. Lastly, the lesions were categorized and documented according to the number of lesions detected by breast ultrasonography (single or multiple), the edge characteristics of the lesion (clear, unclear, spiculated, or with a pseudopodium), and the maximum diameter of the main lesion measured by ultrasound (USmd).

Table 1 Patient basic information

Imaging/pathological features	Training group		Validation group	
	M+ group (*n* = 40)	M- group (*n* = 186)	M+ group (*n* = 17)	M- group (*n* = 80)
Age	56.15 ± 13.54	59.01 ± 10.38	65.87 ± 9 .31	55.98 ± 10.63
Group, *n* (%)				
BCS	19 (47.5)	185 (99.5)	8 (47.1)	78 (97.5)
Non-BCS	21 (52.5)	1 (0.5)	9 (52.9)	2 (2.5)
Molecular subtypes, *n* (%)				
Luminal A	9 (22.5)	64 (34.4)	1 (6.7)	31 (38.8)
Luminal B_ Her2(-)	16 (40.0)	70 (37.6)	8 (47.1)	33 (41.3)
Luminal B_ Her2(+)	5 (12.5)	29 (15.6)	5 (29.4)	9 (11.3)
HER2_ enriched	6 (15.0)	6 (3.2)	2 (11.8)	4 (5.0)
TNBC	4 (10.0)	17 (9.1)	0 (0.0)	3 (3.8)
Tumor size	2.5 (1.1-6.0)	2.08 (0.50-5.40)	2.27 (1.3-5.0)	1.95 (0.80-6.70)

All cases were randomly divided into a training group (226 cases, 69.97%) and a validation group (97 cases, 30.03%). Patients with positive margins in each group belonged to the M+ group, while those with negative margins belonged to the M- group. BCS: Breast-conserving surgery.

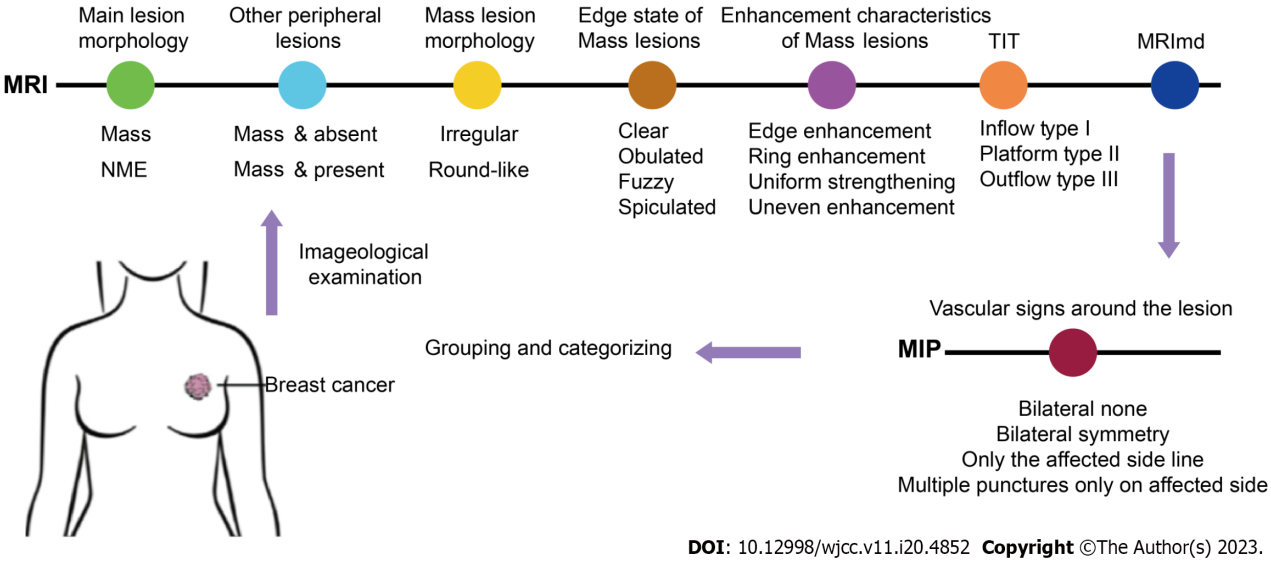

DOI: 10.12998/wjcc.v11.i20.4852

Figure 1 Detailed definition of different feature indicators in magnetic resonance imaging and maximal intensity projection. The patient's magnetic resonance imaging data were classified based on different sub-features, and the patients were grouped and statistically analyzed. MIP: Maximal intensity projection; MRI: Magnetic resonance imaging; NME: Non-mass enhancement.

Mammography examination method and image analysis

The mammography examination utilized a full digital breast DR system (Mmmomat Novation DR, Siemens, Germany) with automatic exposure. The system had a detector size of 35cm × 52 cm × 11 cm and an imaging area size of 24 cm × 29 cm. The maximum image matrix was 3328 × 4096 pixels with a pixel depth of 14-bit. The radiologist assessed the location, shape, size, boundary, and presence of calcification in the lesions during the examination. The lesions were classified based on their shape (mass, irregular density increase, high-density nodular shadow, or no sign) and edge characteristics (blurry, clear, or spiculate). Furthermore, the maximum diameter of the lesion under the molybdenum target (MT-Xmd) was documented.

BCS

Preoperatively, the location and extent of the breast mass were determined based on imaging data obtained from breast ultrasonography, X-ray, or MRI. Neoadjuvant therapy patients had the tumor edge marked with blue dye prior to treatment. A curved incision was made in the upper quadrant and a radial incision in the lower quadrant of the breast.

The skin flap was separated, and the tumor, along with the surrounding breast gland tissue, was excised with a margin of > 1 cm along the palpation boundary. The fascia of the pectoralis major was excised as well. Subsequently, the remaining glandular tissue was reconstructed and modified to facilitate tumor closure. The resected specimen was marked in six directions (upper, lower, inner, outer, surface, and base) for pathological examination using frozen sections.

Pathological examination

The resected specimens were processed in a specific order for edge evaluation through frozen sections to comply with the standards set by the American Pathological Association. Afterward, the specimens were fixed, dehydrated, and embedded in paraffin before being sectioned and stained with hematoxylin and eosin (HE) according to the standard paraffin sectioning procedure. These steps were implemented to ensure a comprehensive examination of the specimens.

Follow-up

For continuous monitoring of the patient's condition, a combination of telephone and mail follow-ups was employed, with one follow-up conducted annually. The latest follow-up was conducted in July 2021.

Statistical analysis

Statistical analysis was performed using SPSS 23.0 software and R software (version 4.0.3). The normality of quantitative data was checked using the Kolmogorov-Smirnov test for single-sample, and for non-normally distributed quantitative data, the median (M) and quartiles (P25, P75) were adopted. A nonparametric rank sum test was conducted for between-group comparisons. For normally distributed quantitative data, mean standard deviation was used, and between-group comparisons were performed using a *t*-test. Count data were presented as frequency and percentage, and the χ^2 test was capitalized for between-group comparisons. The significance level was set at $\alpha = 0.05$.

Single-factor logistic regression analysis was performed to analyze the factors influencing positive surgical margins. The analysis was conducted using the R software package "stata" (version 4.0.3) and "mass" package (version 7.3-53)[12-16]. Factors with $P < 0.1$ were assessed for multicollinearity using the "stata" software package. In cases of multicollinearity, LASSO regression screening was performed using the "glmnet" package of R software (version 4.0-2). The optimal LASSO regression model was constructed by selecting the Lambda (λ) value with the smallest standard error. The regression factors with non-zero coefficients identified by the LASSO regression model were then included in the multiple logistic regression model[17].

The R software package "rms" (version 6.1-0) was utilized to assign scores to each value level of the predictive factors with non-zero regression coefficients screened out by LASSO regression according to the degree of the influence of each factor on the outcome variable in the regression model, and the individual scores were then summed to obtain a total score. Finally, a column line chart illustrating the probability of a positive surgical margin predicted by the total score was generated. The chart was created using the function transformation relationship between the total score and the probability of a positive surgical margin[18].

The receiver operating characteristic (ROC) curve of the total score predicting positive surgical margin was plotted using the R software package "pROC" (version 1.16.2). The area under the ROC curve (AUC) was also calculated[19].

RESULTS

Basic information of included patients

The study included a total of 323 female breast cancer patients who met the inclusion and exclusion criteria. The patients were randomly assigned to either a training group (226 cases, 69.97%) or a validation group (97 cases, 30.03%). The training group had an age range of 31-80 years, with an average age of 58.51 years, while the validation group had an age range of 37-81 years, with an average age of 58.33 years. There was no statistically significant difference between the two groups (see Table 1). Patients were categorized into two groups, namely the margin-positive group (M+) and the margin-negative group (M-), based on intraoperative frozen section pathology and postoperative pathological results. The margin-negative group consisted of 266 cases (186 cases in the training group and 80 cases in the control group), while the margin-positive group comprised 57 cases (40 cases in the training group and 17 cases in the control group). Out of these cases, 2 cases were initially diagnosed as margin-negative by frozen section pathology but later confirmed as margin-positive by postoperative pathological examination. Additionally, 12 cases showed positive results in both the first and second intraoperative frozen section pathology, while 13 cases were negative. Breast conservation surgery was successful in 290 cases, while 33 cases were considered failures, resulting in a breast conservation success rate of 89.78%.

Comparison of MRI, X-ray mammography, ultrasound, and pathological results of patients

A comprehensive analysis was conducted on the data of 323 patients to evaluate the diagnostic value of various preoperative data for margin positivity. Risk factor analysis was performed using the chi-square test for inter-group comparison, and the results are presented in Table 2. The initial focus was on the MRI diagnosis of the training group, which revealed that differentiating the main lesion shape on dynamic contrast-enhanced breast MRI was not effective in predicting margin positivity compared to margin-negative patients. Significant differences were observed in various shapes, including NME, mass, mass with NME, and mass with mass, between the margin-positive and margin-negative groups. This suggests a lack of characteristic main lesion shapes for differentiation. However, other features, such as the presence of multiple punctate vascular signs around the lesion, tumor diameter greater than 2 cm, and a type III time

Table 2 Comparison of clinical and pathological characteristics among different patients

Imaging/pathological features	Training group				Validation group			
	M+group (*n* = 40)	M- group (*n* = 186)	Statistical value	*P* value	M+ group (*n* = 17)	M- group (*n* = 80)	Statistical value	*P* value
Age	56.154 ± 13.537	59.008 ± 10.378	0.063	0.200	65.87 ± 9.31	55.98 ± 10.63	0.08	0.20
Group								
BCS	19 (47.5)	185 (99.5)	χ^2 = 66.874	< 0.001	8 (47.1)	78 (97.5)	χ^2 = 29.32	< 0.001
Non-BCS	21 (52.5)	1 (0.5)			9 (52.9)	2 (2.5)		
MRI								
Lesion type								
Mass	15 (37.5)	87 (46.8)	χ^2 = 42.153	< 0.001	8 (47.1)	54 (67.5)	χ^2 = 12.782	< 0.001
NME	1 (2.5)	11 (5.9)	χ^2 = 19.263	< 0.001	0 (0)	1 (12.5)	χ^2 = 1.191	0.275
Mass + NME	8 (20.0)	38 (20.4)	χ^2 = 14.719	< 0.001	3 (17.6)	6 (75.0)	χ^2 = 3.525	0.060
Mass + Mass	16 (40.0)	50 (26.9)	χ^2 = 8.847	0.003	6 (35.3)	14 (17.5)	χ^2 = 1.794	0.180
MIP_TRA								
Linear	10 (25.0)	76 (40.9)	χ^2 = 0.816	0.366	1 (5.9)	26 (32.5)	χ^2 = 1.575	0.209
Multiple punctate	18 (45.0)	4 (2.2)	χ^2 = 34.67	< 0.001	8 (47.0)	4 (5.0)	χ^2 = 1.166	0.280
Symmetric	5 (12.5)	27 (14.5)	χ^2 = 0.687	0.407	3 (5.9)	8 (10.0)	χ^2 < 0.001	1.000
None	7 (17.5)	79 (42.5)	χ^2 = 2.986	0.084	5 (29.4)	42 (52.5)	χ^2 < 0.001	1.000
Enhancement								
Heterogeneous	29 (72.5)	146 (78.5)	χ^2 = 0.039	0.843	16 (86.7)	59 (73.8)	χ^2 = 0.554	0.457
Homogeneous	8 (20.0)	29 (15.6)	χ^2 = 0.075	0.784	1 (6.7)	17 (21.3)	χ^2 = 0.760	0.383
Rim enhancement	3 (7.5)	11 (5.9)	χ^2 = 0.005	0.942	0 (6.7)	4 (5.0)	χ^2 < 0.001	1.000
Tumor size	2.5 (1.1, 6.0)	2.08 (0.50, 5.40)	0.099	0.001	2.27 (1.3, 5.0)	1.95 (0.80, 6.70)	χ^2 = 0.751	< 0.001
Time_Intensity_Curve								
Type I	3 (7.5)	29 (15.6)	χ^2 = 1.619	0.203	2 (11.8)	20 (25.0)	χ^2 < 0.001	1.000
Type II	7 (17.5)	61 (32.8)	χ^2 = 0.078	0.780	8 (47.1)	25 (31.3)	χ^2 = 0.133	0.715
Type III	30 (75.0)	96 (51.6)	χ^2 = 20.197	< 0.001	7 (41.2)	35 (43.8)	χ^2 = 0.512	0.474
Margin								
Clear	3 (7.5)	21 (11.29)	χ^2 < 0.001	1.000	2 (11.8)	10 (12.5)	χ^2 = 0.025	0.875
Unclear	8 (20.0)	28 (15.05)	χ^2 = 0.028	0.868	5 (29.4)	16 (20.0)	χ^2 = 0.088	0.767
Spiculated	29 (72.5)	137 (73.66)	χ^2 = 0.089	0.766	10 (58.8)	54 (67.5)	χ^2 < 0.001	1.000
Shape								
Irregular	30 (75)	111 (59.7)	χ^2 = 0.294	0.588	14 (82.4)	53 (66.3)	χ^2 = 7.335	0.007
Roundish	5 (12.5)	59 (31.7)	χ^2 = 0.545	0.460	3 (17.6)	19 (23.8)	χ^2 = 5.058	0.025
Multiple nodules	5 (12.5)	16 (8.6)	χ^2 < 0.001	1.000	0 (0.0)	8 (10.0)	χ^2 = 0.301	0.583
MT								
Tumor shape								
High_Density_Nodule	1 (2.5)	9 (4.8)	χ^2 < 0.001	1.000	0 (0.0)	8 (10.0)	χ^2 < 0.001	1.000
Regular mass	21 (52.5)	113 (60.8)	χ^2 = 3.436	0.064	13 (76.5)	46 (57.5)	χ^2 = 9.529	0.002
Irregular mass	3 (7.5)	35 (18.8)	χ^2 = 0.056	0.813	4 (23.5)	13 (16.3)	χ^2 = 11.054	0.001
Undetected	15 (37.5)	29 (15.6)	χ^2 = 5.565	0.018	2 (11.8)	13 (16.3)	χ^2 = 235	0.628

Margin								
Clear	6 (15.0)	24 (12.9)	$\chi^2 = 1.108$	0.292	3 (17.6)	13 (16.3)	$\chi^2 = 0.590$	0.442
Unclear	10 (25.0)	83 (44.6)	$\chi^2 < 0.001$	0.993	7 (41.2)	37 (46.3)	$\chi^2 < 0.001$	1.000
Spiculated	9 (22.5)	62 (33.3)	$\chi^2 = 0.436$	0.509	5 (29.4)	24 (30.0)	$\chi^2 < 0.001$	1.000
Undetected	15 (37.5)	17 (9.14)	$\chi^2 = 5.565$	0.018	2 (11.8)	6 (7.50)	$\chi^2 = 0.235$	0.628
US								
Margin								
Clear	18 (45.0)	55 (29.6)	$\chi^2 = 0.604$	0.437	3 (17.6)	19 (23.8)	$\chi^2 = 0.117$	0.733
Unclear	10 (25.0)	72 (38.7)	$\chi^2 = 1.084$	0.298	9 (52.9)	40 (50.0)	$\chi^2 = 0.001$	0.977
Spiculated	9 (22.5)	59 (31.7)	$\chi^2 = 0.096$	0.756	5 (29.4)	21 (26.3)	$\chi^2 = 0.009$	0.926
Multifocality								
Multifocality	10 (25.0)	29 (9.0)	$\chi^2 = 0.383$	0.536	4 (23.5)	10 (12.5)	$\chi^2 < 0.001$	1.000
Univocality	30 (75.0)	157 (91.0)			13 (76.5)	70 (87.5)		
ER								
Positive	31 (77.5)	163 (87.6)	$\chi^2 = 4.866$	0.027	15 (88.2)	71 (88.8)	$\chi^2 = 0.301$	0.583
Negative	9 (22.5)	23 (12.4)			2 (11.8)	9 (11.3)		
PR								
Positive	30 (73.1)	145 (78.0)	$\chi^2 = 0.864$	0.353	14 (82.4)	67 (83.8)	$\chi^2 = 0.295$	0.587
Negative	10 (26.9)	41 (22.0)			3 (17.6)	13 (16.3)		
Molecular subtypes								
Luminal A	9 (22.5)	64 (34.4)	$\chi^2 = 0.545$	0.460	1 (6.7)	31 (38.8)	$\chi^2 = 0.643$	0.423
LuminalB_Her2(-)	16 (40.0)	70 (37.6)	$\chi^2 = 0.152$	0.696	8 (47.1)	33 (41.3)	$\chi^2 = 2.363$	0.124
LuminalB_Her2(+)	5 (12.5)	29 (15.6)	$\chi^2 = 0.410$	0.522	5 (29.4)	9 (11.3)	$\chi^2 < 0.001$	1.000
HER2_enriched	6 (15.0)	6 (3.2)	$\chi^2 = 9.549$	0.002	2 (11.8)	4 (5.0)	$\chi^2 < 0.001$	1.000
TNBC	4 (10.0)	17 (9.1)	$\chi^2 = 0.008$	0.928	0 (0.0)	3 (3.8)	$\chi^2 = 0.089$	0.766

BCS: Breast-conserving surgery; MIP: Maximal intensity projection; NME: Non-mass enhancement; MRI: Magnetic resonance imaging; US: Ultrasound; MT: Molybdenum target examination; ER: Estrogen receptor; PR: Progesterone receptor.

signal intensity curve, aided in predicting margin positivity. Furthermore, other preoperative data, such as invisible tumors and unclear margin in X-ray mammography, unclear margin in ultrasound examination, and estrogen receptor (ER) positivity and HER2 amplification in immunohistochemistry, were identified as risk factors for margin positivity (Table 2).

LASSO regression

LASSO regression was utilized to identify the most influential factors for constructing a predictive model for breast conservation success. A column line plot predictive model was constructed using four predictive factors: ER status, Mo Xmd Shape, MIP-TRA, and Lesion Type on MRI, to predict negative margins. The ROC curve of the training group revealed an AUC value of 0.919 (95%CI: 0.746-0.962) for predicting successful breast conservation. The calibration curve for internal validation in the training set confirmed the consistency between the actual negative margins and the predicted results of the column line plot. Figure 2 presents the final predictive model, while Figure 2E and F displays the ROC curve and calibration curve, respectively.

Subsequently, we validated the column chart model using the patient data harvested from the control group as a validation set. The ROC curve for the validation set column exhibited an AUC value of 0.701 (95%CI: 0.708-0.733) for predicting successful breast conservation (Figure 3A). The ROC curve for the column demonstrated an AUC value of 0.785 (95%CI: 0.679-0.857) for predicting failure in breast conservation (Figure 3B). Notably, the model for predicting breast conservation failure was not applied separately to the training and validation sets due to the limited number of cases, particularly in terms of breast conservation failure. The internal validation calibration curve for the validation set demonstrated the consistency between the actual negative margin and the column chart prediction (Figure 3C). These findings suggest that the four predictive factors identified through LASSO regression [ER status, molybdenum target tumor type (MT Xmd Shape), MIP-TRA, and lesion type on MRI] hold substantial predictive value for negative margins and the probability of successful breast conservation.

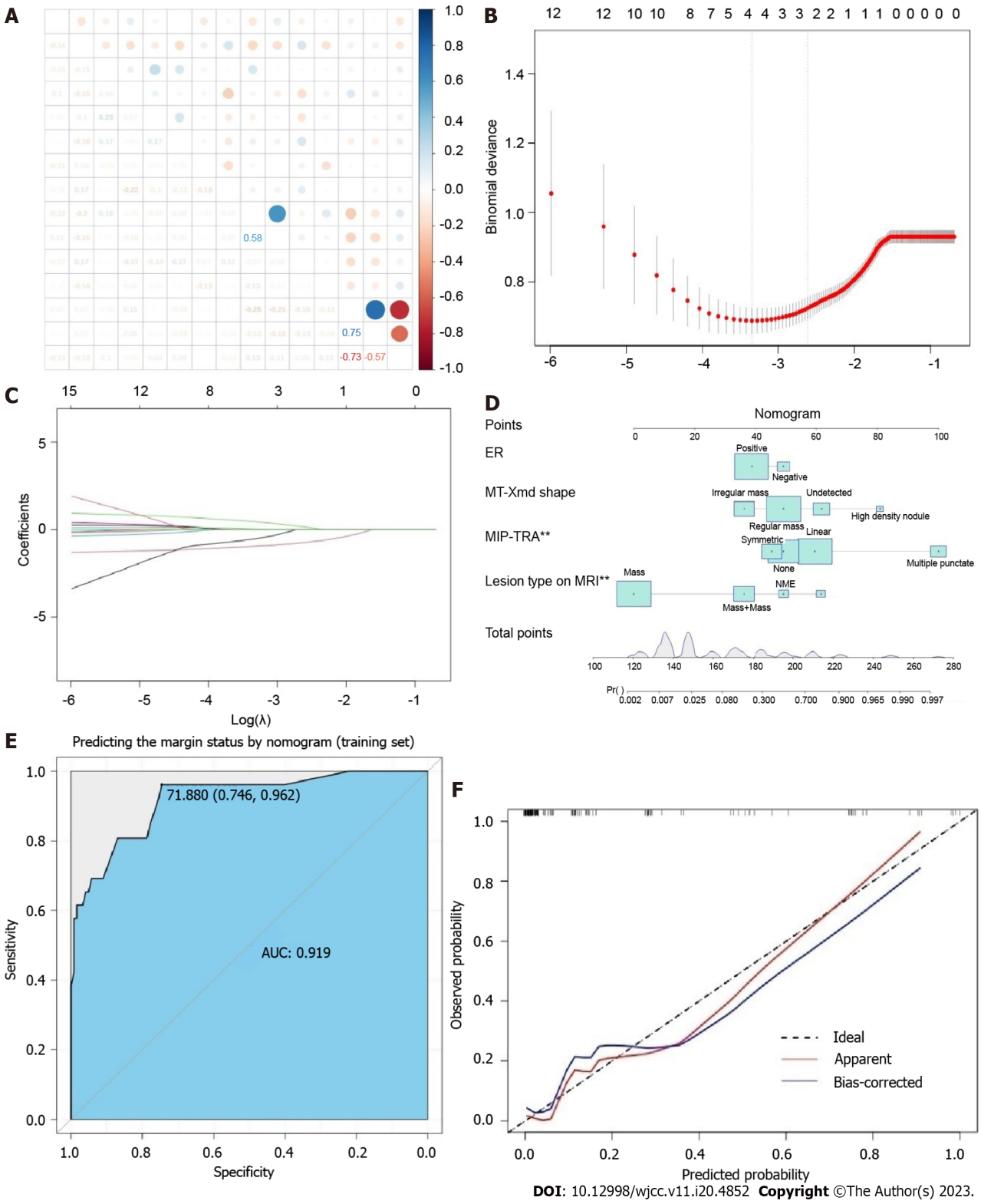

DOI: 10.12998/wjcc.v11.i20.4852

Figure 2 Selected predictive factors and predicted negative margins. A: The "stata" software package determined the presence of multicollinearity among the factors influencing negative margins; B: The best parameter (λ) was selected in the LASSO model, and a vertical dashed line was drawn at the optimal value. The red dot represents the target variable for each λ, and two dashed lines represent special λ values; C: From the 12 identified non-zero coefficient influencing factors, each curve represents the trajectory of one factor's change. The vertical axis is the value of the coefficient, the horizontal axis below is log (λ), and the horizontal axis above is the number of non-zero coefficients in the model at this time; D: Column line chart prediction model for predicting negative margins; E: Column line receiver operating characteristic curve for predicting negative margins in the training cohort; F: Internal validation calibration curve for the training set. MIP: Maximal intensity projection; NME: Non-mass enhancement.

DISCUSSION

Numerous clinical studies have demonstrated that increasing the extent of surgical resection does not necessarily

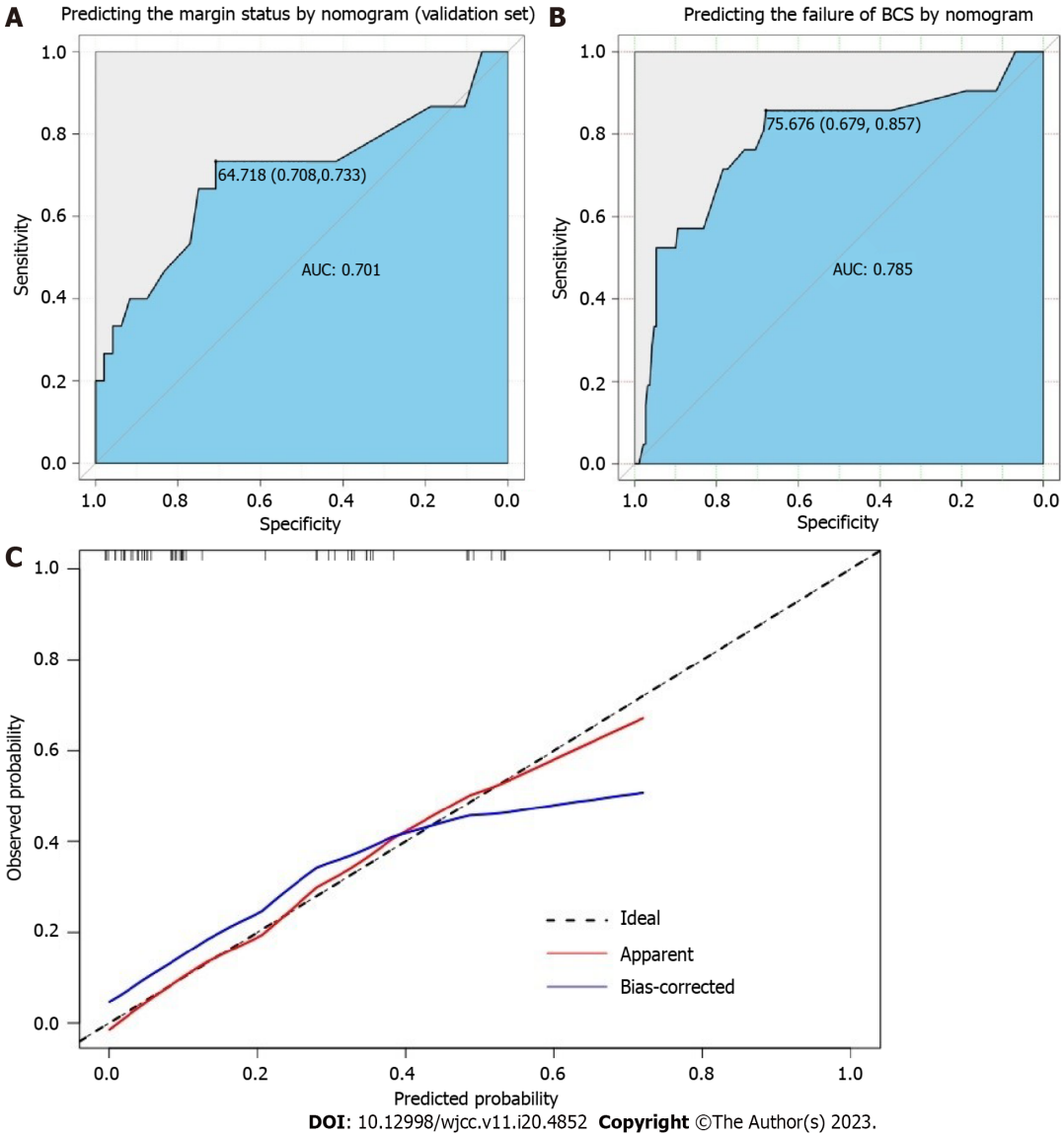

DOI: 10.12998/wjcc.v11.i20.4852

Figure 3 Validation cohort nomogram prediction model constructed using the predictive factors selected by LASSO regression for predicting negative surgical margins. A: Nomogram receiver operating characteristic (ROC) curve for predicting successful breast conservation in the validation cohort; B: Nomogram ROC curve for predicting failed breast conservation (the model for predicting failed breast conservation was not separated by the training and validation groups due to the small number of cases in the study); C: Internal validation calibration curve in the validation cohort. BCS: Breast-conserving surgery.

improve patient survival rates. Additionally, surgeries frequently result in postoperative complications that impact the patient's quality of life. In contrast, BCS entails the removal of the tumor while preserving a significant portion of the breast tissue, followed by radiotherapy and chemotherapy as cancer treatments. Our approach has demonstrated efficacy in curing cancer with minimal physical and psychological trauma for women. Consequently, BCS has emerged as the preferred surgical choice for early-stage breast cancer patients, enabling them to preserve the natural appearance of their breasts. Available data indicate that young breast cancer patients have shown a preference for BCS in China, making it the standard surgical treatment for early-stage breast cancer patients[3,20].

Nonetheless, the substantial incidence of local recurrence following BCS poses a major hurdle to its advancement. Toubou *et al*[21] performed BCS in 528 cases of stage I and II breast cancer. Among them, 176 cases utilized tamoxifen for a minimum of 2 years, while 116 cases underwent chemotherapy for at least 6 cycles. These patients exhibited 5-year and 10-year local recurrence rates of 7% and 14%, respectively. In Holland's study of 129 patients who underwent local tumor excision with cancer-negative pathological margins, a local recurrence rate of 9.3% on the ipsilateral side of the breast was observed[22]. Numerous studies have investigated factors associated with local recurrence following BCS, encompassing patient-related factors, tumor diameter, lymph node metastasis, vascular and nerve involvement, as well as the presence of preoperative neoadjuvant chemotherapy and histopathological type[23-25]. Among these factors, the surgical treatment method holds particular significance, especially in cases where the margin pathology indicator is positive during BCS, as it serves as a pivotal factor indicating the likelihood of local recurrence post-surgery[26,27].

To ensure negative surgical margins, a meta-analysis by Houssami *et al*[28] in 2014 found that "No ink on tumor" can serve as the best negative margin for BCS, and increasing margin width beyond this point does not reduce the risk of local recurrence. Consequently, the American Society of Surgical Oncology and the American Society for Radiation Oncology has established "No ink on tumor" as a safe margin for BCS in patients with invasive breast cancer who undergo postoperative whole-breast radiation therapy[29]. Regarding ductal carcinoma in situ of the breast, the guidelines specify that a margin within 2 mm of the surgical incision, devoid of tumors, is deemed negative[30]. Nevertheless, certain research findings indicate the presence of residual tumors even after re-excising margin specimens measuring less than 2 mm[31,32]. Therefore, enhancing preoperative imaging assessment is crucial to accurately establish a safe margin range.

Breast ultrasound and mammography are widely employed as diagnostic and screening methods for breast cancer. Nevertheless, breast ultrasound has limitations in detecting non-mass type breast cancer, resulting in reduced sensitivity and specificity. Moreover, interpreting ultrasound images is a subjective process that demands a high level of professional expertise, particularly in cases of multifocal or multicenter breast cancer. Depending solely on ultrasound examination for preoperative evaluation can lead to missed diagnoses. Conversely, mammography involves compressing and deforming the breast to acquire a two-dimensional overlapping image of the breast tissue, affecting the glandular density and potentially masking small lesions within the overlapping images. Previous studies have reported relatively low sensitivity and accuracy of breast ultrasound and mammography in detecting non-mass type breast cancer. In addition, the accuracy of routine ultrasound and mammography for diagnosing multifocal or multicenter breast cancer is low, and the positive margin rate and failure rate of BCS are high. Therefore, improving preoperative imaging assessment is crucial for accurately determining the extent of the lesion and ensuring negative surgical margins.

Breast MRI offers high-resolution soft tissue imaging and better approximates the natural drooping state of the breast during examinations, mitigating compression-induced alterations in lesion location and size. MRI examination allows for detailed observation of lesion morphology, enhancement characteristics, blood supply, as well as the condition of other areas of the breast. Furthermore, the comprehensive assessment of multiple sequence images can enhance the accuracy of tumor invasion prediction and ultimately improve the success rate of BCS. Breast MRI exhibits a sensitivity of over 90% in detecting invasive breast cancer[33-37]. The American College of Radiology has classified the morphology and characteristics of lesions in detail in the BI-RADS MR system[3]. Based on this, the author simplified the classification of lesion morphology. The study showed that in MRI examinations, the surgical margin positive rate of mass-type lesions with other lesions present (Mass & present) and non-mass type enhancement lesions (NME) around the lesion was higher than that of mass-type lesions without other lesions present (Mass & absent), which indicates that BCS may be more suitable for Mass & absent type breast cancer, and more attention should be given when choosing BCS for patients with the first two types of breast cancer. Moreover, the presence of multiple nodular signs around the lesion in the MIP image of MRI is a risk factor for positive surgical margins. Dietzel *et al*[38] confirmed that the adjacent vessel sign (AVS) was more prevalent in malignant lesions than in benign lesions, demonstrating a specificity of 88% and a positive predictive value of 85%. In addition, compared to invasive ductal carcinoma, AVS was less frequent in situ carcinoma (27% *vs* 54%), suggesting a correlation between AVS signs and tumor infiltration into surrounding tissue.

This study identified four predictive factors through LASSO regression: the positive status of ER, the type of tumor detected by molybdenum target, MIP-TRA, and the type of tumor detected by MRI. These factors hold greater significance in predicting negative surgical margins. However, ultrasound, tumor size, and margin morphology detected by molybdenum target examination were not correlated with positive surgical margins. Small breast volume is additionally linked to positive margins in BCS. Therefore, imaging characteristics far from the lesion are considered a risk factor for positive margins in BCS.

This study has several limitations as well. Firstly, the retrospective nature of the study raises concerns regarding potential selection bias and confounding factors. Secondly, the substantial variation in sample size between groups due to the high success rate of BCS as per current guidelines may impact the generalizability of the findings. Thirdly, the sample size of some subcategories, such as HER-2 amplification, was relatively small, potentially limiting the statistical power of the analysis. Therefore, more data is needed to further validate the results. Fourthly, the omission of pathological factors in the analysis of BCS success may have restricted the comprehensiveness of the study. Lastly, the study had a relatively small sample size, warranting the need for a larger sample size to assess the accuracy of the model.

CONCLUSION

In this retrospective study, data from enrolled patients, including ultrasound, mammography, MRI, and biopsy results, were analyzed. A nomogram model was constructed to predict the likelihood of success for BCS. This study identified ER-positive status, mammography tumor type, MIP-TRA, and MRI tumor type as four predictive variables that can influence the success of BCS by determining negative margins. The results underwent internal validation and were additionally confirmed using calibration curves, which revealed a robust correlation between the predicted and actual rates of surgical success. In conclusion, this study offers valuable data that can aid in the preoperative evaluation of BCS outcomes.

ARTICLE HIGHLIGHTS

Research background

Breast cancer is a prevalent malignancy among women, and surgical treatment remains a widely employed approach. However, the presence of positive margins following surgery frequently results in cancer recurrence and metastasis, significantly impacting the treatment outcome and patient prognosis.

Research motivation

With the continuous improvement of medical technology, the treatment of breast cancer is becoming increasingly comprehensive, yet positive margins leading to recurrence and metastasis remain important factors affecting the treatment effect and patient prognosis.

Research objectives

This study aims to investigate the diagnostic value of various preoperative examination methods for breast cancer margin status.

Research methods

A retrospective study was conducted on 323 breast cancer patients who met the criteria for undergoing breast-conserving surgery (BCS). Data on preoperative imaging, as well as intraoperative and postoperative pathological findings, were collected. The patients were categorized into groups based on the presence of positive or negative margins. The data were randomly split into a training set and a validation set. Non-conditional logistic regression and LASSO regression were applied to the validation set to identify risk factors associated with the failure of BCS.

Research results

The presence of non-mass enhancement on magnetic resonance imaging (MRI), indistinct margins on ultrasound and molybdenum target examination, as well as tumor size larger than 2 cm, were identified as factors that elevate the risk of positive margins.

Research conclusions

The model utilizes preoperative evaluation results from ultrasound, molybdenum target, MRI, and core needle biopsy pathology, all of which were aligned with the actual situation. This provides reliable guidance for clinical decision-making concerning BCS.

Research perspectives

This study established a computational model to forecast the success of BCS using variables such as ER-positive status, mammography tumor type, maximum intensity projection imaging feature, and MRI tumor type. This has significant implications for preoperative evaluation and the selection of appropriate surgical interventions, thus improving surgical success rates and negative margin rates.

FOOTNOTES

Author contributions: Liu P and Kang H designed the study; Liu P, Zhao Y, and Rong DD wrote the manuscript; Liu P, Li KF, and Zhao J performed the experiments; Zhao Y, Rong DD and Wang YJ analyzed the data; Hua Kang reviewed and revised the manuscript; all authors have read and approved the final manuscript.

Institutional review board statement: The study was reviewed and approved by the Ethics Committee of Xuanwu Hospital, Capital Medical University.

Informed consent statement: The data used in this study were not related to the patients' privacy information, so the informed consent was waived by the Ethics Committee of Xuanwu Hospital, Capital Medical University. All data obtained, recorded, and managed were only used for this study, without any harm to the patients.

Conflict-of-interest statement: All the authors report no relevant conflicts of interest for this article.

Data sharing statement: No additional data are available.

Country/Territory of origin: China

ORCID number: Peng Liu 0009-0006-4015-644X; Hua Kang 0009-0000-1130-6417.

S-Editor: Yan JP
L-Editor: A
P-Editor: Zhao S

REFERENCES

1 **Bray F**, Ferlay J, Soerjomataram I, Siegel RL, Torre LA, Jemal A. Global cancer statistics 2018: GLOBOCAN estimates of incidence and mortality worldwide for 36 cancers in 185 countries. *CA Cancer J Clin* 2018; **68**: 394-424 [PMID: 30207593 DOI: 10.3322/caac.21492]

2 **Fisher B**, Anderson S, Bryant J, Margolese RG, Deutsch M, Fisher ER, Jeong JH, Wolmark N. Twenty-year follow-up of a randomized trial comparing total mastectomy, lumpectomy, and lumpectomy plus irradiation for the treatment of invasive breast cancer. *N Engl J Med* 2002; **347**: 1233-1241 [PMID: 12393820 DOI: 10.1056/NEJMoa022152]

3 **Litière S**, Werutsky G, Fentiman IS, Rutgers E, Christiaens MR, Van Limbergen E, Baaijens MH, Bogaerts J, Bartelink H. Breast conserving therapy versus mastectomy for stage I-II breast cancer: 20 year follow-up of the EORTC 10801 phase 3 randomised trial. *Lancet Oncol* 2012; **13**: 412-419 [PMID: 22373563 DOI: 10.1016/S1470-2045(12)70042-6]

4 **Eccles SA**, Aboagye EO, Ali S, Anderson AS, Armes J, Berditchevski F, Blaydes JP, Brennan K, Brown NJ, Bryant HE, Bundred NJ, Burchell JM, Campbell AM, Carroll JS, Clarke RB, Coles CE, Cook GJ, Cox A, Curtin NJ, Dekker LV, Silva Idos S, Duffy SW, Easton DF, Eccles DM, Edwards DR, Edwards J, Evans D, Fenlon DF, Flanagan JM, Foster C, Gallagher WM, Garcia-Closas M, Gee JM, Gescher AJ, Goh V, Groves AM, Harvey AJ, Harvie M, Hennessy BT, Hiscox S, Holen I, Howell SJ, Howell A, Hubbard G, Hulbert-Williams N, Hunter MS, Jasani B, Jones LJ, Key TJ, Kirwan CC, Kong A, Kunkler IH, Langdon SP, Leach MO, Mann DJ, Marshall JF, Martin L, Martin SG, Macdougall JE, Miles DW, Miller WR, Morris JR, Moss SM, Mullan P, Natrajan R, O'Connor JP, O'Connor R, Palmieri C, Pharoah PD, Rakha EA, Reed E, Robinson SP, Sahai E, Saxton JM, Schmid P, Smalley MJ, Speirs V, Stein R, Stingl J, Streuli CH, Tutt AN, Velikova G, Walker RA, Watson CJ, Williams KJ, Young LS, Thompson AM. Critical research gaps and translational priorities for the successful prevention and treatment of breast cancer. *Breast Cancer Res* 2013; **15**: R92 [PMID: 24286369 DOI: 10.1186/bcr3493]

5 **Zhang L**, Jiang M, Zhou Y, Du XB, Yao WX, Yan X, Jiang Y, Zou LQ. Survey on breast cancer patients in China toward breast-conserving surgery. *Psychooncology* 2012; **21**: 488-495 [PMID: 21322089 DOI: 10.1002/pon.1922]

6 **Soerjomataram I**, Lortet-Tieulent J, Parkin DM, Ferlay J, Mathers C, Forman D, Bray F. Global burden of cancer in 2008: a systematic analysis of disability-adjusted life-years in 12 world regions. *Lancet* 2012; **380**: 1840-1850 [PMID: 23079588 DOI: 10.1016/S0140-6736(12)60919-2]

7 **McCahill LE**, Single RM, Aiello Bowles EJ, Feigelson HS, James TA, Barney T, Engel JM, Onitilo AA. Variability in reexcision following breast conservation surgery. *JAMA* 2012; **307**: 467-475 [PMID: 22298678 DOI: 10.1001/jama.2012.43]

8 **Landercasper J**, Whitacre E, Degnim AC, Al-Hamadani M. Reasons for re-excision after lumpectomy for breast cancer: insight from the American Society of Breast Surgeons Mastery(SM) database. *Ann Surg Oncol* 2014; **21**: 3185-3191 [PMID: 25047472 DOI: 10.1245/s10434-014-3905-1]

9 **Takahashi H**, Oshi M, Asaoka M, Yan L, Endo I, Takabe K. Molecular Biological Features of Nottingham Histological Grade 3 Breast Cancers. *Ann Surg Oncol* 2020; **27**: 4475-4485 [PMID: 32436191 DOI: 10.1245/s10434-020-08608-1]

10 **Satoh Y**, Kawamoto M, Kubota K, Murakami K, Hosono M, Senda M, Sasaki M, Momose T, Ito K, Okamura T, Oda K, Kuge Y, Sakurai M, Tateishi U, Fujibayashi Y, Magata Y, Yoshida T, Waki A, Kato K, Hashimoto T, Uchiyama M, Kinuya S, Higashi T, Machitori A, Maruno H, Minamimoto R, Yoshinaga K. Clinical practice guidelines for high-resolution breast PET, 2019 edition. *Ann Nucl Med* 2021; **35**: 406-414 [PMID: 33492646 DOI: 10.1007/s12149-021-01582-y]

11 **Rao AA**, Feneis J, Lalonde C, Ojeda-Fournier H. A Pictorial Review of Changes in the BI-RADS Fifth Edition. *Radiographics* 2016; **36**: 623-639 [PMID: 27082663 DOI: 10.1148/rg.2016150178]

12 **Zanotel M**, Bednarova I, Londero V, Linda A, Lorenzon M, Girometti R, Zuiani C. Automated breast ultrasound: basic principles and emerging clinical applications. *Radiol Med* 2018; **123**: 1-12 [PMID: 28849324 DOI: 10.1007/s11547-017-0805-z]

13 **Woods RW**, Sisney GS, Salkowski LR, Shinki K, Lin Y, Burnside ES. The mammographic density of a mass is a significant predictor of breast cancer. *Radiology* 2011; **258**: 417-425 [PMID: 21177388 DOI: 10.1148/radiol.10100328]

14 **Chiarelli AM**, Edwards SA, Prummel MV, Muradali D, Majpruz V, Done SJ, Brown P, Shumak RS, Yaffe MJ. Digital compared with screen-film mammography: performance measures in concurrent cohorts within an organized breast screening program. *Radiology* 2013; **268**: 684-693 [PMID: 23674784 DOI: 10.1148/radiol.13122567]

15 **Zneimer SM**, Hongo D. Preparing for Clinical Laboratory Improvement Amendments (CLIA) and College of American Pathologists (CAP) Inspections. *Curr Protoc* 2021; **1**: e324 [PMID: 34958716 DOI: 10.1002/cpz1.324]

16 **Masoumi S**, Shahraz S. Meta-analysis using Python: a hands-on tutorial. *BMC Med Res Methodol* 2022; **22**: 193 [PMID: 35820854 DOI: 10.1186/s12874-022-01673-y]

17 **Candia J**, Tsang JS. eNetXplorer: an R package for the quantitative exploration of elastic net families for generalized linear models. *BMC Bioinformatics* 2019; **20**: 189 [PMID: 30991955 DOI: 10.1186/s12859-019-2778-5]

18 **Eng KH**, Schiller E, Morrell K. On representing the prognostic value of continuous gene expression biomarkers with the restricted mean survival curve. *Oncotarget* 2015; **6**: 36308-36318 [PMID: 26486086 DOI: 10.18632/oncotarget.6121]

19 **Robin X**, Turck N, Hainard A, Tiberti N, Lisacek F, Sanchez JC, Müller M. pROC: an open-source package for R and S+ to analyze and compare ROC curves. *BMC Bioinformatics* 2011; **12**: 77 [PMID: 21414208 DOI: 10.1186/1471-2105-12-77]

20 **Meric F**, Mirza NQ, Vlastos G, Buchholz TA, Kuerer HM, Babiera GV, Singletary SE, Ross MI, Ames FC, Feig BW, Krishnamurthy S, Perkins GH, McNeese MD, Strom EA, Valero V, Hunt KK. Positive surgical margins and ipsilateral breast tumor recurrence predict disease-specific survival after breast-conserving therapy. *Cancer* 2003; **97**: 926-933 [PMID: 12569592 DOI: 10.1002/cncr.11222]

21 **Touboul E**, Buffat L, Belkacémi Y, Lefranc JP, Uzan S, Lhuillier P, Faivre C, Huart J, Lotz JP, Antoine M, Pène F, Blondon J, Izrael V, Laugier A, Schlienger M, Housset M. Local recurrences and distant metastases after breast-conserving surgery and radiation therapy for early breast cancer. *Int J Radiat Oncol Biol Phys* 1999; **43**: 25-38 [PMID: 9989511 DOI: 10.1016/s0360-3016(98)00365-4]

22 **Holland PA**, Gandhi A, Knox WF, Wilson M, Baildam AD, Bundred NJ. The importance of complete excision in the prevention of local recurrence of ductal carcinoma in situ. *Br J Cancer* 1998; **77**: 110-114 [PMID: 9459154 DOI: 10.1038/bjc.1998.17]

23 **Mirza NQ**, Vlastos G, Meric F, Buchholz TA, Esnaola N, Singletary SE, Kuerer HM, Newman LA, Ames FC, Ross MI, Feig BW, Pollock RE, McNeese M, Strom E, Hunt KK. Predictors of locoregional recurrence among patients with early-stage breast cancer treated with breast-conserving therapy. *Ann Surg Oncol* 2002; **9**: 256-265 [PMID: 11923132 DOI: 10.1007/BF02573063]

24 **Simpson DJ**, Allan J, McFall B. Factors predicting residual disease on re-excision after breast conserving surgery. *Surgeon* 2022; **20**: e149-e157 [PMID: 34326010 DOI: 10.1016/j.surge.2021.06.003]

25 **Mechera R**, Viehl CT, Oertli D. Factors predicting in-breast tumor recurrence after breast-conserving surgery. *Breast Cancer Res Treat* 2009; **116**: 171-177 [PMID: 18815880 DOI: 10.1007/s10549-008-0187-y]

26 **Choi N**, Kim K, Shin KH, Kim Y, Moon HG, Park W, Choi DH, Kim SS, Ahn SD, Kim TH, Chun M, Kim YB, Kim S, Choi BO, Kim JH. Malignant and borderline phyllodes tumors of the breast: a multicenter study of 362 patients (KROG 16-08). *Breast Cancer Res Treat* 2018; **171**: 335-344 [PMID: 29808288 DOI: 10.1007/s10549-018-4838-3]

27 **Vos EL**, Gaal J, Verhoef C, Brouwer K, van Deurzen CHM, Koppert LB. Focally positive margins in breast conserving surgery: Predictors, residual disease, and local recurrence. *Eur J Surg Oncol* 2017; **43**: 1846-1854 [PMID: 28688723 DOI: 10.1016/j.ejso.2017.06.007]

28 **Houssami N**, Macaskill P, Marinovich ML, Dixon JM, Irwig L, Brennan ME, Solin LJ. Meta-analysis of the impact of surgical margins on local recurrence in women with early-stage invasive breast cancer treated with breast-conserving therapy. *Eur J Cancer* 2010; **46**: 3219-3232 [PMID: 20817513 DOI: 10.1016/j.ejca.2010.07.043]

29 **Moran MS**, Schnitt SJ, Giuliano AE, Harris JR, Khan SA, Horton J, Klimberg S, Chavez-MacGregor M, Freedman G, Houssami N, Johnson PL, Morrow M. Society of Surgical Oncology-American Society for Radiation Oncology consensus guideline on margins for breast-conserving surgery with whole-breast irradiation in stages I and II invasive breast cancer. *Int J Radiat Oncol Biol Phys* 2014; **88**: 553-564 [PMID: 24521674 DOI: 10.1016/j.ijrobp.2013.11.012]

30 **Morrow M**, Van Zee KJ, Solin LJ, Houssami N, Chavez-MacGregor M, Harris JR, Horton J, Hwang S, Johnson PL, Marinovich ML, Schnitt SJ, Wapnir I, Moran MS. Society of Surgical Oncology-American Society for Radiation Oncology-American Society of Clinical Oncology Consensus Guideline on Margins for Breast-Conserving Surgery With Whole-Breast Irradiation in Ductal Carcinoma In Situ. *J Clin Oncol* 2016; **34**: 4040-4046 [PMID: 27528719 DOI: 10.1200/JCO.2016.68.3573]

31 **Merrill AL**, Coopey SB, Tang R, McEvoy MP, Specht MC, Hughes KS, Gadd MA, Smith BL. Implications of New Lumpectomy Margin Guidelines for Breast-Conserving Surgery: Changes in Reexcision Rates and Predicted Rates of Residual Tumor. *Ann Surg Oncol* 2016; **23**: 729-734 [PMID: 26467458 DOI: 10.1245/s10434-015-4916-2]

32 **Peterson ME**, Schultz DJ, Reynolds C, Solin LJ. Outcomes in breast cancer patients relative to margin status after treatment with breast-conserving surgery and radiation therapy: the University of Pennsylvania experience. *Int J Radiat Oncol Biol Phys* 1999; **43**: 1029-1035 [PMID: 10192351 DOI: 10.1016/s0360-3016(98)00519-7]

33 **Akashi-Tanaka S**, Sato N, Ohsumi S, Kimijima I, Inaji H, Teramoto S, Akiyama F. Evaluation of the usefulness of breast CT imaging in delineating tumor extent and guiding surgical management: a prospective multi-institutional study. *Ann Surg* 2012; **256**: 157-162 [PMID: 22751517 DOI: 10.1097/SLA.0b013e31825b6cb1]

34 **Narod SA**, Sun P, Wall C, Baines C, Miller AB. Impact of screening mammography on mortality from breast cancer before age 60 in women 40 to 49 years of age. *Curr Oncol* 2014; **21**: 217-221 [PMID: 25302030 DOI: 10.3747/co.21.2067]

35 **Lai HW**, Chen CJ, Lin YJ, Chen SL, Wu HK, Wu YT, Kuo SJ, Chen ST, Chen DR. Does Breast Magnetic Resonance Imaging Combined With Conventional Imaging Modalities Decrease the Rates of Surgical Margin Involvement and Reoperation?: A Case-Control Comparative Analysis. *Medicine (Baltimore)* 2016; **95**: e3810 [PMID: 27258520 DOI: 10.1097/MD.0000000000003810]

36 **Millet I**, Pages E, Hoa D, Merigeaud S, Curros Doyon F, Prat X, Taourel P. Pearls and pitfalls in breast MRI. *Br J Radiol* 2012; **85**: 197-207 [PMID: 22128131 DOI: 10.1259/bjr/47213729]

37 **Maxwell AJ**, Lim YY, Hurley E, Evans DG, Howell A, Gadde S. False-negative MRI breast screening in high-risk women. *Clin Radiol* 2017; **72**: 207-216 [PMID: 27932250 DOI: 10.1016/j.crad.2016.10.020]

38 **Dietzel M**, Baltzer PA, Vag T, Herzog A, Gajda M, Camara O, Kaiser WA. The adjacent vessel sign on breast MRI: new data and a subgroup analysis for 1,084 histologically verified cases. *Korean J Radiol* 2010; **11**: 178-186 [PMID: 20191065 DOI: 10.3348/kjr.2010.11.2.178]

Published by **Baishideng Publishing Group Inc**
7041 Koll Center Parkway, Suite 160, Pleasanton, CA 94566, USA
Telephone: +1-925-3991568
E-mail: bpgoffice@wjgnet.com
Help Desk: https://www.f6publishing.com/helpdesk
https://www.wjgnet.com